Tetrahedron 66 (2010) 6990–7000

Contents lists available at ScienceDirect

Tetrahedron

journal homepage: www.elsevier.com/locate/tet

1-Aminoanthracene-9,10-dione based chromogenic molecular sensors: effect of nature and number of nitrogen atoms on metal ion sensing behavior

Kuljit Kaur, Subodh Kumar *

Department of Chemistry, Guru Nanak Dev University, Amritsar 143 005, Punjab, India

ARTICLE INFO

Article history:
Received 28 November 2009
Received in revised form 10 June 2010
Accepted 12 June 2010
Available online 17 June 2010

Keywords:
1-Aminoanthracene-9,10-dione
Chemosensors
Selective
Semi-selective
Chromogenic
Heavy metal ions

ABSTRACT

To examine the consequences of nature and number of nitrogen atoms on metal ion sensing properties, four new molecular receptors based on 1-aminoanthracene-9,10-dione as chromogenic moiety and different types of nitrogen atoms viz. arylamine, alkylamine, and pyridyl nitrogen as appendages have been synthesized. These receptors in CH_3OH/H_2O (1:1) (v/v) at pH 7.0, on addition of heavy metal ions show selective and/or semi-selective interactions. These binding interactions are visible to naked eye due to remarkable color change and are associated with λ_{max} shift by 85–125 nm. Molecular receptor **2**, with two sp^2 hybridized nitrogen atoms and one arylamine nitrogen, selectively binds with Cu^{2+} but 2-Cu^{2+} complex is stable only between pH 7.0 and 8.75. However, the conversion of imine nitrogen to alkylamine in molecular receptor **6**, increases the binding ability toward Cu^{2+} along with significant binding affinities toward Ni^{2+} and Co^{2+}. Receptor **6** shows the stability of its complexes in the order $Cu^{2+}>Ni^{2+}>Co^{2+}$ in a broader pH range 6–12. Dipicolylamine based receptor **8**, possessing two pyridyl nitrogen atoms, one tertiaryamine and one arylamine nitrogen atoms as ligating sites, also binds semiselectively in the order $Cu^{2+}>Co^{2+}>Ni^{2+}$. Receptor **10**, possessing anilide group in the place of arylamine in receptor **8**, on addition of Cu^{2+}, Ni^{2+} or Co^{2+} shows bathochromic shift of λ_{max} associated with color change from yellow to russet (brown) and on addition of Zn^{2+} shows hypsochromic shift of its λ_{max} associated with disappearance of yellow color. Additionally, all the four chemosensors show ratiometric response toward all these metal ions and thus increase the usability and the dynamic range of estimation.

1. Introduction

The development of artificial receptors for the sensing and recognition of environmentally and biologically important ionic species is currently of great interest. Highly selective cation[1] or anion[2] sensing is imperative for many areas of technology, including environmental, biological, clinical, and waste management applications. One of the Nature's methods of molecular recognition that has been underexplored by synthetic chemists is differential binding. By differential rather than specific or selective, we refer to receptors that have different binding characteristics. This is the binding scenario used in the mammalian senses of taste and smell. Nature does not use highly selective receptors for each analyte in the senses of taste and smell,[3] and instead uses an array of differential receptor units, which come into play on demand.

As an alternative strategy to traditional analyte specific receptors the contemporary investigations are addressing to the development of the sensor molecules that operate on a single core receptor unit for multi-ion analysis.[4–6] The paradigm shift from selective to differential receptors has provided opportunities for single molecule based simultaneous estimation of more than one analyte by single detection method. The production of differential receptors for analytes has bright future for the field of recognition in the area of molecular sensing. The number of examples of such sensors have been reported[4] and tend to use either the insertion of multi chromogenic units combined in a single receptor[5,7] or a variety of detection methods[6] (fluorescence, electrochemical) or require detailed mathematical tools to process the data.

The drastic color change ensuing in metal induced deprotonation at amine NH has recently found applications in developing single or multi-ion sensing materials. Qian et al.[7] in naphthalimide based sensors have shown NH deprotonation as the key step for estimation of Cu^{2+} using both absorbance and fluorescence as output channels. Our group has investigated a number of metal ion sensors with chromogenic anthracene-9,10-dione moiety bearing a variety of appendages at 1-, 1,4-, and 1,8-positions.[8] These chromogenic chemosensors with amines as appendages bind only with Cu^{2+} in a highly selective manner[8a–d] or with dipyridyl amino ethyl[8e] or Schiff base[8f] as appendages at 1-position of anthracene-9,10-dione showed semi-selective/differential complexation

* Corresponding author. Tel.: +91 0183 2258802; fax: +91 0183 2258820; e-mail address: subodh_gndu@yahoo.co.in (S. Kumar).

0040-4020/$ – see front matter © 2010 Elsevier Ltd. All rights reserved.
doi:10.1016/j.tet.2010.06.031

toward Cu^{2+} and Ni^{2+} or toward Cu^{2+} and Ni^{2+}/Co^{2+}. Recently, Guilard et al.[9] has reported anthracene-9,10-dione based macrocycles, which showed semi-selectivity for Cu^{2+}, Al^{3+}, and Pb^{2+} by changing the environment of nitrogen atoms of ligating sites in the macrocycles.

In our continued search for the semi-selective metal ion sensors, here we have designed four molecular receptors **2**, **6**, **8**, and **10** possessing arylamine, alkylamine, imine or pyridyl nitrogen atoms in various combinations and have studied their interactions toward metal ions in CH_3OH/H_2O (1:1) at pH 7.0. The receptors **2**, **6**, **8**, and **10** are by and large silent to the presence of alkali and alkaline earth metal ions. However in the presence of heavy metal ions, they show remarkable color changes with Cu^{2+}, Ni^{2+} or Co^{2+} in a selective or in a semi-selective manner. The stability of these complexes is sensitive to pH under different pH ranges depending on the nature of the binding sites. The chemosensor **2** (λ_{max} 494 nm) having arylamine and two C=N– nitrogen atoms (Py and imine N's) underwent a drastic color change from red to blue only on addition of Cu^{2+} (λ_{max} 604 nm)—a selective chromogenic chemosensor for Cu^{2+}. Chemosensor **6** (λ_{max} 500 nm) with change in hybridisation of one nitrogen from sp^2 to sp^3 exhibited characteristic color changes on the addition of Co^{2+}, Ni^{2+} (λ_{max} 626 nm) and Cu^{2+} (λ_{max} 604 nm). Receptor **8** (λ_{max} 518 nm) with two pyridyl rings, one alkylamine and one arylamine as ligating sites also showed remarkable color changes with Co^{2+}(λ_{max} 636 nm), Ni^{2+} (λ_{max} 666 nm), and Cu^{2+} (λ_{max} 624 nm). Chemosensor **10** having anilide moiety in place of the arylamine moiety in chemosensor **8** showed dual mode of complexation toward metal ions. The λ_{max} of chemosensor **10** (λ_{max} 400 nm) on addition of Co^{2+}, Ni^{2+} (λ_{max} 488 nm), and Cu^{2+} (λ_{max} 484 nm) was bathochromically shifted to give russet color but on addition of Zn^{2+} (λ_{max} 367 nm) it was hypsochromically shifted[7c] and the yellow color of **10** disappeared to give colorless solution.

2. Results and discussion

2.1. Synthesis

The refluxing of 1:1 solution of 1-(2-aminoethylamino) anthracene-9,10-dione (**1**)[8a] and pyridine-2-carboxaldehyde in ethanol gave chemosensor **2** (80%), red solid. The presence of 1H singlet at δ 8.48 due to imine=CH along with other signals in the aromatic region due to anthracene-9,10-dione and pyridine moieties confirms the formation of Schiff base. Its ^{13}C NMR and mass spectral data and elemental analysis further confirm the structure **2** for this compound (Scheme 1).

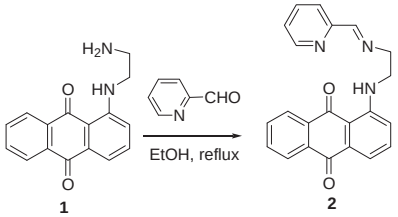

Scheme 1.

Chemosensors **6** and **8** have been synthesized by mesylation of 1-(2-hydroxyethylamino)-anthracene-9,10-dione **3** with methanesulfonyl chloride followed by nucleophilic substitution with 2-picolylamine (**5**) and di-(2-picolyl)amine (**7**) (Scheme 2).

The reaction of **3** with methanesulphonyl chloride in DCM in the presence of triethylamine provided **4** (80%), red solid. In its ^1H NMR spectrum the presence of a 3H singlet at δ 3.09 due to methanesulfonyl moiety and down field shift of OCH_2 triplet to δ 4.49 in

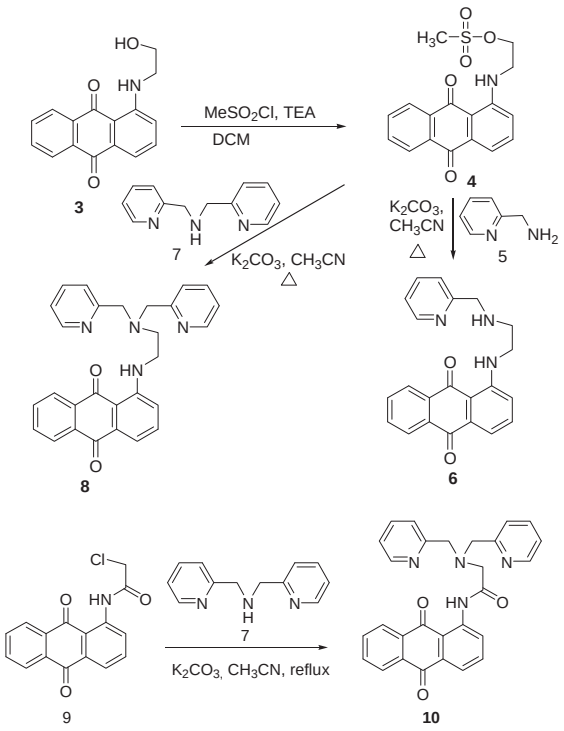

Scheme 2.

comparison to the one appeared in **3** at δ 3.76 confirm that alcohol moiety has been converted to its methanesulfonyl ester. The presence of other signals in its ^1H NMR spectrum and its ^{13}C spectral data further confirm the structure **4** for this compound.

The nucleophilic substitution of **4** with 2-picolylamine (**5**) in K_2CO_3/CH_3CN provided **6** (65%), dark red solid. Its ^1H NMR spectrum shows two 2H triplets at δ 3.06 (CH_2) and at δ 3.50 (CH_2) and a 2H singlet at δ 4.03 (CH_2), respectively, due to ethylene and NCH_2Py groups along with signals in the aromatic region at δ 7.08 (dd, 1H), 7.15–7.19 (1H, m), 7.41 (1H,d), 7.50–7.61 (2H, m), 7.66–7.79 (3H, m), 8.25 (1H, d), 8.29 (1H, d), 8.54–8.56 (1H, m). These spectral data along with ^{13}C NMR spectral data and elemental analysis corroborate the structure **6** for this compound (Scheme 2).

Compound **4** on nucleophilic substitution with di-(2-picolyl) amine (**7**) in K_2CO_3/CH_3CN provided **8** (60%), red solid. In its ^1H NMR spectrum the presence of a 4H singlet at δ 4.06 along with 2H triplet at δ 2.96 and a 2H quartet at δ 3.45 in the aliphatic region along with signals in the aromatic region due to both anthracene-9,10-dione and pyridine moieties confirm the formation of compound **8**.

Compound **9**[10] on nucleophilic substitution with di-(2-picolyl) amine (**7**) in K_2CO_3/CH_3CN solution gave chemosensor **10** (75%), yellow solid. In its ^1H NMR spectrum the presence of two singlets at δ 3.54 (2H) and at δ 4.06 (4H) along with presence of signals in the aromatic region due to anthracene-9,10-dione and pyridine moieties confirm the formation of the compound (Scheme 2).

2.2. Effect of metal ions on absorption properties of chemosensors 2, 6, 8, and 10

The interactions of chemosensors **2**, **6**, **8**, and **10** with metal ions have been investigated by evaluating the changes in their absorption properties by the addition of different metal ions. These chemosensors are freely soluble in methanol/water (1:1), so all investigations have been performed in CH_3OH/H_2O (1:1) at pH 7.0 (10 mM HEPES).

The visible region absorption band of chemosensor **2** (50 μM) appeared at λ_{max} 494 nm (red), which on addition of Cu^{2+} (50 μM) underwent an immediate visible color change from red to blue. This color change is associated with the decrease in absorbance at 494 nm and concomitant appearance of new absorption band at 604 nm. Significantly, **2** did not undergo any color change or change in absorbance on addition of other metal ions like Na^{+}, K^{+}, Mg^{2+}, Ca^{2+}, Ba^{2+}, Cr^{3+}, Co^{2+}, Ni^{2+}, Zn^{2+}, Cd^{2+}, Hg^{2+}, Ag^{+}, and Pb^{2+}. Therefore, chemosensor **2** showed selective estimation of Cu^{2+} (Figs. 1a and 2a).

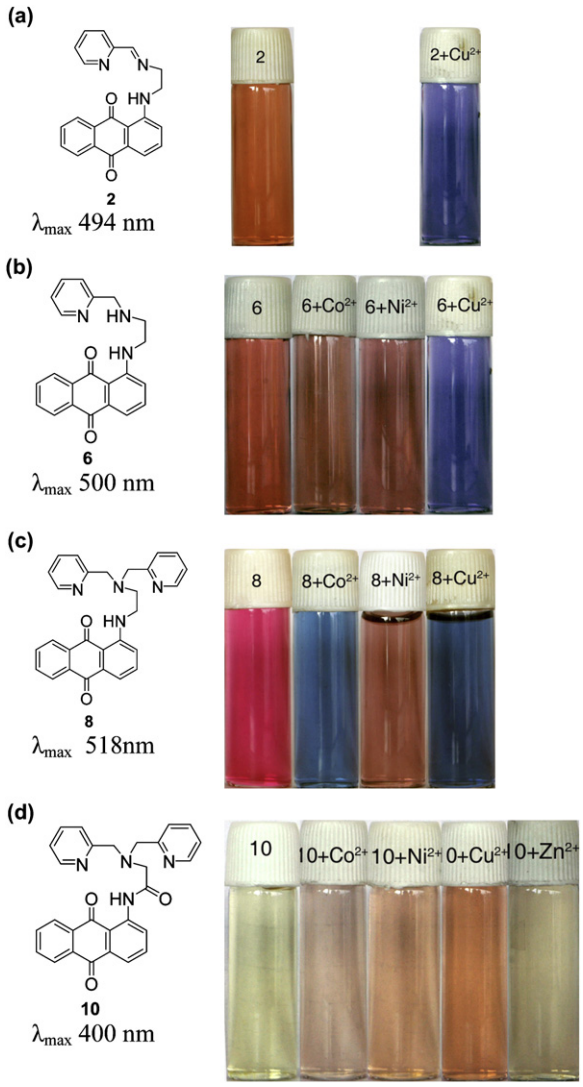

Figure 1. Color changes in chemosensors **2**, **6**, **8**, and **10** (50 μM; CH_3OH/H_2O 1:1) on addition of different metal ions.

Chemosensor **6**, where the imine moiety present in chemosensor **2** has been reduced to amine with a change in hybridisation of nitrogen from sp^2 to sp^3, exhibited λ_{max} at 500 nm, which underwent a color change from red to blue in case of Cu^{2+} (604 nm), lilac in case of Co^{2+} and Ni^{2+} (626 nm). The other metal ions like Na^{+}, K^{+}, Mg^{2+}, Ca^{2+}, Ba^{2+}, Cd^{2+}, Zn^{2+}, Hg^{2+}, Ag^{+} etc. cause negligible responses to the absorption spectrum of **6**. Therefore the conversion of sp^2 N in the chemosensor **2** to sp^3 N in chemosensor **6** increases the binding ability of resulting chemosensor toward metal ions (Figs. 1b and 2b).

Chemosensor **8** (λ_{max} 518 nm) with an additional pyridine ring as binding unit as compared with chemosensor **6** on addition of

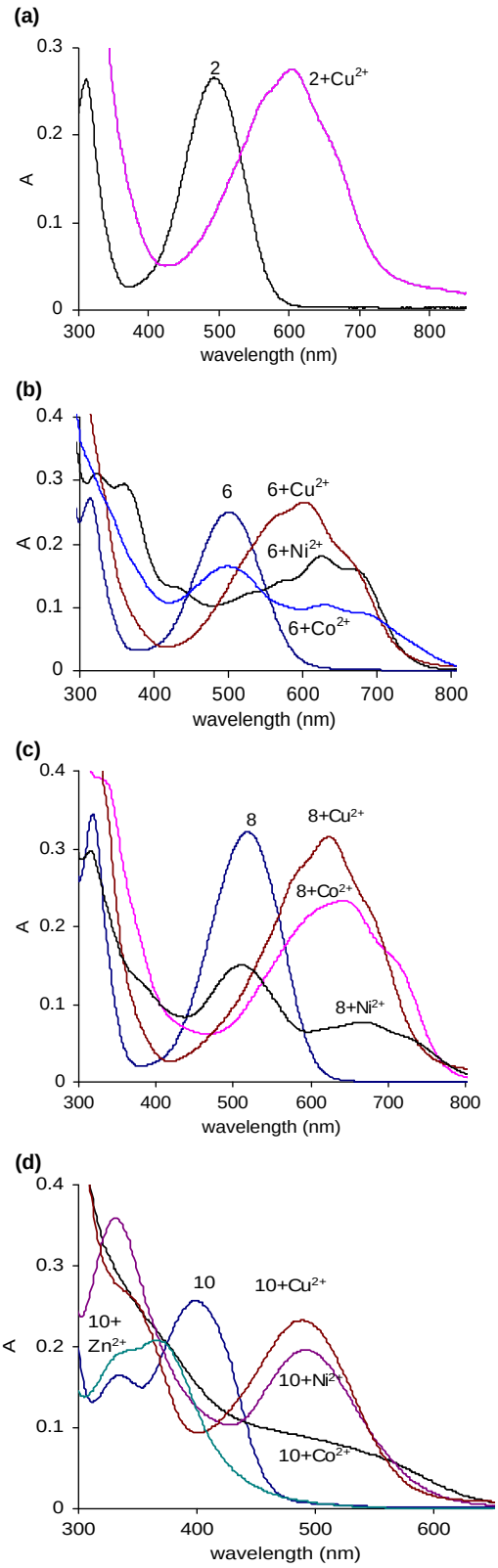

Figure 2. Changes in the UV–vis spectra (50 μM; pH 7.0±0.1; CH_3OH/H_2O 1:1) on addition of metal ions (a) **2** (b) **6** (c) **8**, and (d) **10**.

Cu^{2+} (624 nm) and Co^{2+} (636 nm) gave dark blue color and on addition of Ni^{2+} gave purple color (666 nm). The addition of other metal ions to the solution of **8** did not affect its color or absorption spectrum (Figs. 1c and 2c).

The presence of an electron-withdrawing carbonyl group on N-1 nitrogen of **10**, decreases the ICT from nitrogen lone pair to the anthracene-9,10-dione ring and thus caused 118 nm hypsochromic shift to λ_{max} 400 nm in comparison to **8** (λ_{max} 518 nm). The solution of chemosensor **10** appeared yellow, which on addition of Cu^{2+} (484 nm), Co^{2+} and Ni^{2+} (488 nm) showed bathochromic shift (~84 nm) associated with color change to russet (Figs. 1d and 2d).

However, addition of Zn^{2+} to **10** caused hypsochromic shift to 367 nm with concomitant color change from yellow to nearly colorless (Fig. 1d). So, amongst chemosensors studied here, only **10** shows complexation toward Zn^{2+}.

The chemosensors **2**, **6**, and **8** have $RNCH_2CH_2NH$ unit at N-1 of anthracene-9,10-dione moiety with different nitrogen containing groups appended on chain. Although these appended nitrogen containing moieties are not directly attached to anthracene-9,10-dione moiety but considerably affect their λ_{max} values. These variations in λ_{max} values could be assigned to through space interactions of lone pair of electrons of appended nitrogen atoms with π-cloud of 1-aminoanthracene-9,10-dione moiety. The conversion of sp^2 hybridised nitrogen in **2** to sp^3 hybridised nitrogen in **6** makes the lone pair of electrons more easily available for interaction with π-cloud and thus causes 6 nm bathochromic shift of λ_{max} to 500 nm. In the case of chemosensor **8**, the presence of additional pyridine nitrogen increases the contribution of through space interactions and thus leads to further bathochromic shift of λ_{max} at 500 nm to 518 nm.

2.3. Effect of pH on absorption spectra of 2, 6, 8, and 10 and their complexes with metal ions

In order to evaluate the effect of pH on protonation behavior of chemosensors **2**, **6**, **8**, and **10**, the solutions of these chemosensors (50 μM) in CH_3OH/H_2O (1:1) were titrated with NaOH and HCl solutions separately and the effect was measured by recording UV–vis spectra at different pH values. The spectral data thus obtained were analysed using an iterative method on multi-wavelength data using the programme specfit/32.

Chemosensor **2** showed changes in its absorption and λ_{max} values on changing pH from 2 to 12 (Fig. 3). The absorption maxima of **2** appeared at 494 nm at pH≤7 and shifted to 514 nm at pH≥9. The analysis of the pH induced changes in the spectrum of **2** using iterative spectral fitting shows that at pH≥9, **2** exists in monoprotonated and neutral forms but at pH≤7, it exists in di- and triprotonated forms (for log β values see Table 1).

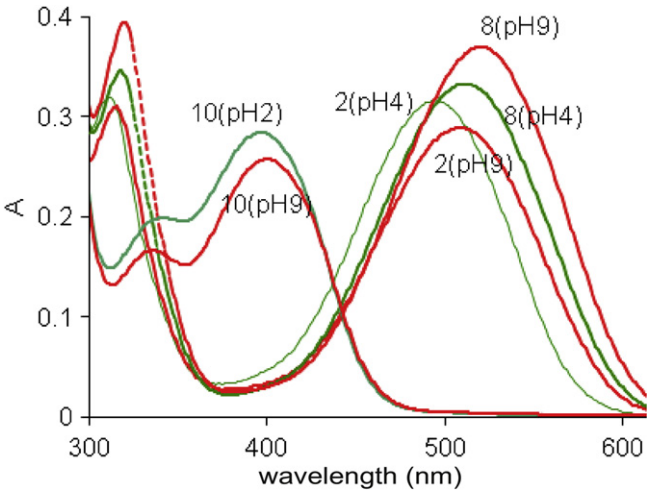

Figure 3. Changes in the UV–vis spectra of chemosensors **2**, **8**, and **10** (50 μM; CH_3OH/H_2O 1:1) on pH variation.

Table 1
Protonation constants of chemosensors **2**, **6**, **8**, **10** in CH_3OH/H_2O (1:1)

Chemosensor	log β_{LH}	log $\beta_{LH\ 2}$	log β_{LH3}
2	11.1±0.1	19.8±0.1	23.9±0.1
6	9.59±0.1	16.62±0.1	20.57±0.1
8	8.39±0.1	13.79±0.1	17.64±0.2
10	8.18±0.09	13.00±0.09	15.96±0.13

Similarly, chemosensors **6** and **8** on moving from acidic to basic medium showed respective 10 and 8 nm bathochromic shifts. The analysis of pH induced changes in the spectrum of **8** shows that at pH≥7, chemosensor **8** exists mainly in monoprotonated form. At pH 4.5, the nitrogen atoms of both the pyridine moieties are protonated simultaneously to form triprotonated species.

In case of chemosensor **10**, the analysis of spectral data obtained from pH dependent absorption changes show that mono and diprotonation at tertiaryamine and pyridine nitrogen atoms does not affect the absorption spectrum of free **10** between pH 4 and 9, which could be assigned to the presence of carbonyl electron-withdrawing group at 1-anthrylamine nitrogen. However, further protonation at amide or anthraquinone oxygen atoms at pH<4 causes 4 nm hypsochromic shift.

In order to have insight into effect of pH on the formation of various stoichiometric complexes, the 1:1 mixtures of chemosensors **2**, **6**, **8**, and **10** with different metal ions in CH_3OH/H_2O (1:1) were titrated with NaOH and HCl solutions separately. The decision of taking 1:1 stoichiometric solutions was based on the formation of 1:1 complexes during titration of various receptors against metal ion concentration at pH 7 (discussed in Section 2.4). The spectral data thus obtained was analysed using an iterative method on multi-wavelength data using the programme specfit/32.

The evaluation of spectral data obtained by combination of pH and UV-vis titration of solution of **2**-Cu^{2+} (1:1) (Figs. 4a and 4b) shows that at pH<5, the UV-vis spectrum corresponds to protonated **2** and points to no complexation of **2** with Cu^{2+}. On increasing the pH above 5, the gradual increase in absorbance at 604 nm associated with decrease in absorbance at 494 nm occurs. These observations point to the formation of MLH_{-1} stoichiometric complex, which achieves completion at pH 7 and remains stable upto pH 8.75. On increasing pH above 8.75, the decomplexation of the **2**-Cu^{2+} complex occurs due to formation of $Cu(OH)_2$ and free chemosensor **2**. The formation of free **2** is further ascertained by the increase in absorbance at 494 nm and decrease in absorbance at 604 nm. The negative log β value for $MLH_{-1}(OH^-)$ also points to the instability of MLH_{-1} complex under strong basic conditions.

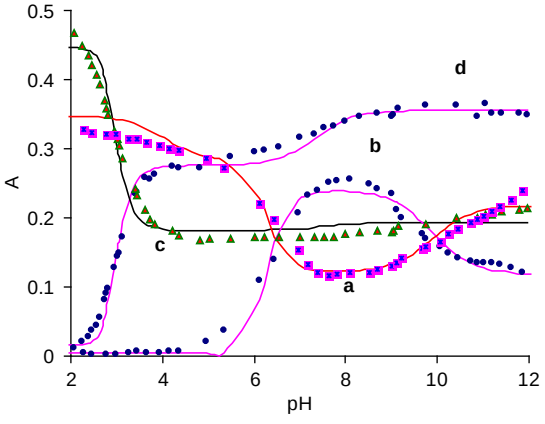

Figure 4. Plot of absorbance of chemosensor-Cu^{2+} (1:1) complex (50 μM; CH_3OH/H_2O 1:1) vs pH. For 2-Cu^{2+} complex (a) at 494 nm, (b) at 604 nm and for **6**-Cu^{2+} complex (c) at 500 nm, (d) at 604 nm. The points refer to experimental values and line to curve fit.

In case of chemosensor **6**, the titration of 1:1 solution of Cu^{2+} and **6** showed the appearance of new absorption band at 604 nm at pH 3, which was associated with decrease in absorbance at 500 nm (Figs. 4c and 4d). These observations point to the complexation of **6** with Cu^{2+} at significantly lower pH. This complexation process was completed at pH 4.0 and remained stable till pH 6.5. On increasing the pH>6.5, the absorbance at 604 nm further increased till it achieved a plateau at pH 8.5 and then remained stable even under strong basic conditions at pH 12. Obviously, at pH<2.5, the chemosensor **6** remains partly protonated and probably one of the amine nitrogen in appendage along with nitrogen at 1-aminoanthraquinone moiety participates in complex formation. As the pH was further increased, the deprotonation of the other nitrogen increased the complexation and thus the absorbance at 604 nm. Due to increased number of binding sites, the complex remained quite stable even under strong basic conditions (for different species formation and log β values see Table 2).

Table 2
log β values obtained by pH titration of 1:1 complexes of chemosensors **2**, **6**, **8**, **10** (CH_3OH/H_2O; 1:1) with various metal ions

L-M^{2+}	ML	MLH	MLH_{-1}	MLH_{-1} OH^-
2-Cu^{2+}	—	—	5.65±0.06	−4.24±0.08
6-Co^{2+}	23.73±0.1	—	20.09±0.09	10.93±0.08
6-Ni^{2+}	—	—	3.25±0.05	—
6-Cu^{2+}	—	—	13.25±0.03	5.91±0.10
8-Co^{2+}			18.87±0.08	11.55±0.05
8-Cu^{2+}	—	29.36±0.16	17.96±0.16	10.04±0.14
10-Co^{2+}	26.83±0.08	30.16±0.11	20.75±0.05	11.59±0.04
10-Ni^{2+}	23.76±0.14	—	18.24±0.06	11.34±0.04
10-Cu^{2+}	26.04±0.1	—	21.08±0.1	11.52±0.1
10-Zn^{2+}	13.64±0.38	16.51±0.39	7.34±0.38	−2.58±0.38

During titration of 1:1 solution of **6**-Co^{2+} complex, the presence of new absorption bands at 626 nm and 691 nm even at pH 2.5 and decrease in absorbance of chemosensor **6** at 500 nm to 0.32 from 0.45 shows that **6** remains complexed with Co^{2+} even at such a low pH. The absorbance of **6**-Co^{2+} complex at 626 nm remains stable between pH 4–9 (Figs. 5a and 5b).

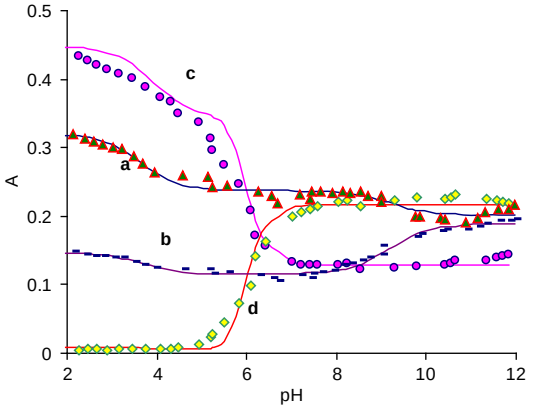

Figure 5. Effect of pH on the absorbance of **6**-Co^{2+} (1:1) and **6**-Ni^{2+} complexes (50 μM; CH_3OH/H_2O 1:1); For **6**-Co^{2+} complex (a) at 500 nm, (b) at 626 nm and for **6**-Ni^{2+} complex (c) at 500 nm, (d) at 626 nm. The points refer to experimental values and line to curve fit.

The evaluation of spectral data obtained by titration of 1:1 solution of **6**-Ni^{2+} shows that **6** starts forming the complex with Ni^{2+} only at pH 5.5 and completes the formation of complex at pH 7.0 (Fig. 5c and d). This complex with MLH_{-1} stoichiometry as determined from multi-wavelength spectral data processing remains stable even under strong basic conditions (up to pH 12).

Therefore, the change in nature of nitrogen atom from sp^2 hybridized in chemosensor **2** to sp^3 hybridized in chemosensor **6** increases the ease in formation and stability of the **6**-Cu^{2+} complex toward hydrolysis under both acidic and basic conditions. **2**-Cu^{2+} complex is stable in pH range 6.5 to 8.5 only whereas **6**-Cu^{2+}, **6**-Ni^{2+}, and **6**-Co^{2+} complexes are stable under broader pH range. The complex formation in both these cases is associated with increased intramolecular charge transfer from N-1 amine to anthracene-9,10-dione moiety.

The evaluation of spectral data obtained by titration of 1:1 solution of **8**-Co^{2+} complex with NaOH and HCl (Fig. 6) shows the strong complexation of **8** with Co^{2+} even under strong acidic conditions. At pH 2.0, the absorption spectrum of **8**-Co^{2+} complex gives a well structured absorption spectrum with three absorption bands at 575, 623, and 680 nm, which on increasing pH above 7.0 appears with bathochromic shift to 600 nm, 654 nm, and 711 nm. The evaluation of spectral data using multi-wavelength data processing shows the formation of MLH_{-1} and $MLH_{-1}(OH^-)$ complexes.

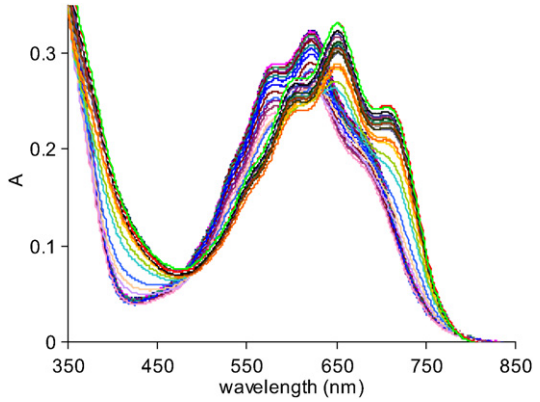

Figure 6. Changes in the UV–vis spectrum of **8**-Co^{2+} complex on changing pH from 2 to 12 (50 μM; CH_3OH/H_2O 1:1).

The pH titration of 1:1 stoichiometric solution of **8** and Cu^{2+} at pH>8 shows stable absorption band at λ_{max} 624 nm, which on lowering the pH gradually decreases with the appearance of new absorption band at 467 nm and achieved plateau at pH<4.5. This λ_{max} at 467 nm is associated with the disappearance of absorption band at 624 nm. During this variation in pH from 12 to 2 there is minimal change in absorbance at λ_{max} 518 nm, i.e., at absorption maxima of chemosensor **8** (Fig. 7). Therefore, **8** undergoes change in mode of complexation while moving from basic to acidic

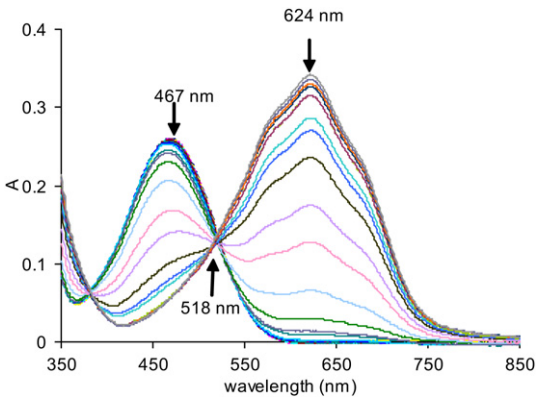

Figure 7. Changes in the UV–vis spectrum of **8**-Cu^{2+} complex on changing pH from 2 to 12 (50 μM; CH_3OH/H_2O 1:1).

medium. At pH 7.00 and above, the complexation of **8** with Cu^{2+} causes deprotonation at anthrylamine N-1 to increase the internal charge transfer from amine N to anthraquinone moiety and thus shows a red shifted absorption band at 624 nm. At pH≤4.5, the coordination of anthrylamine N-1 of chemosensor **8** with Cu^{2+} leads to reverse internal charge transfer from anthryl group to Cu^{2+} and thus shows a blue shifted absorption band at 467 nm.

Similarly, 1:1 stoichiometric solution of **8** and Ni^{2+} on pH titration, at pH>8 shows absorption band at λ_{max} 666 nm, which on lowering the pH gradually decreases with the appearance of new absorption band at 503 nm, which achieved plateau at pH<5.8. This λ_{max} at 503 nm is associated with the disappearance of absorption band 666 nm. During this variation in pH from 12 to 2 an isobestic point appears at 545. Therefore, two species with λ_{max} 666 nm and 503 nm remain in equilibrium with each other between pH 8 and 6. Thus, **8** undergoes change in mode of complexation while moving from basic to acidic medium. At pH 7.00 and above, the complexation of **8** with Ni^{2+} causes deprotonation at anthrylamine N-1 to increase the internal charge transfer and thus shows a bathochromic shifted absorption band at 666 nm. At pH≤5.8, the coordination of anthrylamine N-1 with Ni^{2+} leads to reverse internal charge transfer from anthryl group to Ni^{2+} and thus shows an absorption band with a hypsochromic shift to 503 nm (Fig. 8).

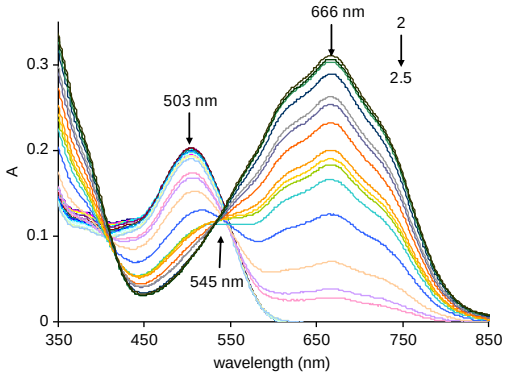

Figure 8. Changes in the UV–vis spectrum of **8**-Ni^{2+} complex on changing pH from 2 to 12 (50 μM; CH_3OH/H_2O 1:1).

The evaluation of spectral data obtained by titration of 1:1 solution of **10**-Cu^{2+} with NaOH and HCl (Fig. 9) shows the strong complexation of **10** with Cu^{2+} under both acidic and basic conditions. Between pH 6.0 and 8.5, mainly the complex of stoichiometry MLH_{-1} exists, which gives bathochromic shifted absorption band with λ_{max} 484 nm. At pH<4, Cu^{2+} forms only a complex with hypsochromic shifted absorption band at 383 nm and

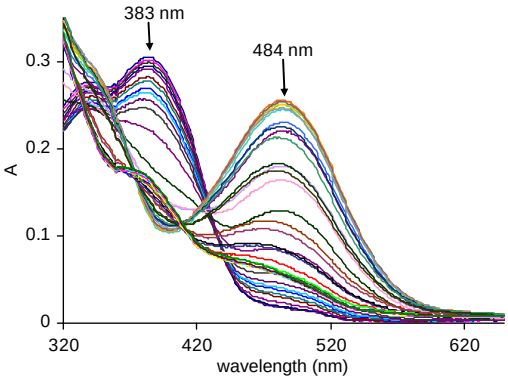

Figure 9. Changes in the UV–Vis spectrum of **10**-Cu^{2+} complex on changing pH from 2 to 12 (50 μM; CH_3OH/H_2O 1:1).

stoichiometry ML. However, at pH>8.5 due to increased hydroxyl ions concentration, the MLH_{-1} complex is relatively less stable and undergoes hydrolysis to give free **10** and $Cu(OH)_2$.

The titration of 1:1 stoichiometric solution of **10** and Ni^{2+} with NaOH and HCl shows that at pH>5, a new absorption band at 488 nm appeared. The intensity of this band increased gradually with increase in pH to 7.0 and then a plateau was achieved. On lowering the pH from 7, a new absorption band at 383 nm appeared (Fig. 10), which achieved plateau at pH 4.5. The spectral fitting of these data obtained by pH—UV–vis. combination titration of **10**-Ni^{2+} (1:1) complex shows that **10** forms ML complex at pH<4 and deprotonation at aromatic NH starts at pH>4, resulting in the formation of MLH_{-1}, which is completed at pH 6. On further increasing pH from 6 formation of $MLH_{-1}(OH^-)$ starts, which is completed at pH 8.0 and remains stable even up to pH 12.

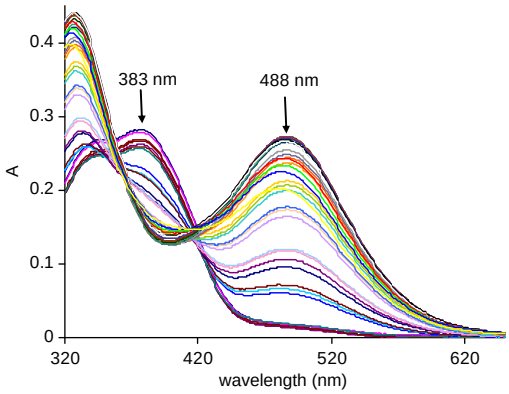

Figure 10. Changes in the UV–Vis spectrum of **10**-Ni^{2+} complex on changing pH from 2 to 12 (50 μM; CH_3OH/H_2O 1:1).

The titration of 1:1 stoichiometric solution of **10** and Zn^{2+} with NaOH and HCl shows that at pH 10, the absorption maxima appears at 394 nm, which on gradual decrease in pH underwent gradual hypsochromic shift to 367 nm (Fig. 11). The analysis of these spectral data using an iterative method on multi-wavelength data shows that depending on pH of the solution various stoichiometric complexes MLH, ML, MLH_{-1}, and $MLH_{-1}(OH^-)$ remain in equilibrium but all the complexes show hypsochromic shift with respect to free chemosensor **10** irrespective of the pH of the solution.

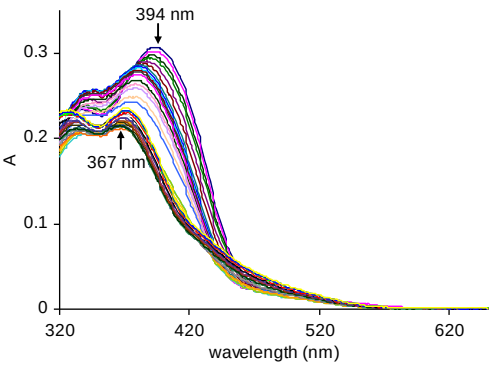

Figure 11. Changes in the UV–Vis spectrum of **10**-Zn^{2+} complex on changing pH from 2 to 12 (50 μM; CH_3OH/H_2O 1:1).

The analysis of spectral data obtained by pH titration of **10**-Co^{2+} complex with NaOH and HCl using an iterative method on multi-wavelength data shows that depending on pH of the solution various stoichiometric complexes MLH, ML, MLH_{-1}, and $MLH_{-1}(OH^-)$ remain in equilibrium (Fig. 12).

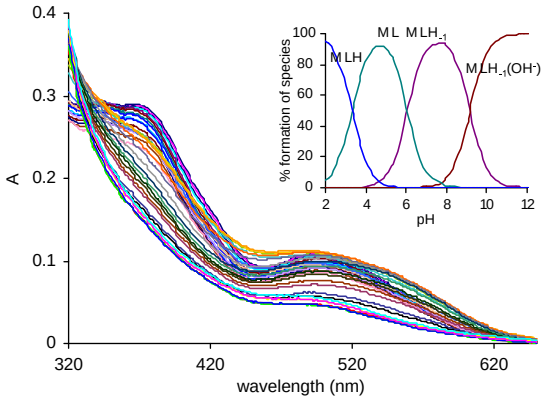

Figure 12. Changes in the UV–vis spectrum of **10**-Co^{2+} complex on changing pH from 2 to 12 (50 μM; CH_3OH/H_2O 1:1). Inset shows the species distribution over pH range 2–12.

Therefore, the presence of additional pyridine unit in chemosensor **8** increases the complexation toward other transition metal ions to Co^{2+}, Ni^{2+}, and Cu^{2+} and also provides pH dependent dual mode of complexation toward Ni^{2+} and Cu^{2+}. Both Cu^{2+} and Ni^{2+} bind chemosensor **8** at pH>6 through ICT from nitrogen to anthracene-9,10-dione ring but at pH≤4, it shifts ICT from N-1 to metal ion which is associated with hypsochromic shift of absorption band.

The presence of an amide unit in chemosensor **10** further increases the opportunities toward alternate mode of complexation. Both Co^{2+} and Zn^{2+} irrespective of pH cause hypsochromic shift of free ligand absorption band. However, in case of complexation of **10** with Cu^{2+} and Ni^{2+}, the mode of complexation switches from ICT from nitrogen to ring at pH>6 to the ICT from nitrogen to metal ion at pH<4.

2.4. Quantitative estimation of metal ions at pH 7

In order to find out the usability of these chemosensors for quantitative estimation of metal ions, the titrations of chemosensors **2**, **6**, **8**, and **10** against metal ions, which gave color/spectral changes as discussed in Section 2.2 were studied.

The titration of **2** (50 μM) with Cu^{2+} at pH 7.0±0.1 (10 mM HEPES in CH_3OH/H_2O 1:1) resulted in the emergence of a new peak at 604 nm. The intensity of absorbance at 604 nm increased gradually with simultaneous decrease in intensity at 494 nm. The presence of two clear isosbestic points at 530 nm and 396 nm confirms the equilibration between **2** and **2**-Cu^{2+} complex at pH 7. The spectral fitting of the titration data shows the formation of 1:1 complex with log β=4.60s±0.04.

On addition of Cu^{2+} to the solution of chemosensor **6** at pH 7, the appearance of a new peak at λ_{max} 604 nm was observed with two isosbestic points at 538 nm and 398 nm. The color of the solution changed from red to blue. The spectral fitting of the data shows the formation of ML (log β=7.67±0.46) and ML_2 (log β=13.27±0.6) stoichiometric complexes. The increased stability of **6**-Cu^{2+} complex by order of 1000 times in comparison to **2**-Cu^{2+} complex is in consonance with increased coordination of alkylamine nitrogen over imine nitrogen and the stability of **6**-Cu^{2+} complex over broader pH range as observed in its pH titration.

The titration of solution of chemosensor **6** with Co^{2+} or Ni^{2+} in separate experiments gave new absorption bands with λ_{max} 626 nm and two isosbestic points at 430 nm and 559 nm. In each case ML_2 and ML stoichiometric species are formed. The log β values have been given in Table 3.

The titration of chemosensor **8** against Co^{2+} showed the appearance of a new peak at 636 nm with two clear isosbestic points at 435 nm and 564 nm (Fig. 13). The intensity of absorption at λ_{max} 636 nm increased gradually with increase in concn of Co^{2+}. The spectral fitting of the data shows the formation of ML (log β=7.74±0.63) stoichiometric complex.

Table 3
Stability constants of chemosensors **2**, **6**, **8**, and **10** (50 μM, CH_3OH/H_2O 1:1) with metal ions at pH 7±0.1

Chemosensor	Metal ion	Stability constant
2	Cu^{2+}	ML (log β=4.60±0.04)
6	Co^{2+}	ML (log β=6.68±0.29)
		ML_2 (log β=12.76±0.37)
		ML_3 (log β=18.10±0.39)
	Ni^{2+}	ML (log β=7.92±0.45)
		ML_2 (log β=13.13±0.59)
	Cu^{2+}	ML (log β=7.67±0.46)
		ML_2 (log β=13.27±0.60)
8	Co^{2+}	ML (log β=7.74±0.63)
	Ni^{2+}	ML (log β=7.52±0.5)
		ML_2(log β=12.63±0.8)
	Cu^{2+}	ML (log β=7.27±0.37)
10	Co^{2+}	ML (log β=7.65±0.25)
		M_2L (log β=13.15±0.38)
	Ni^{2+}	ML (log β=5.92±0.08)
	Cu^{2+}	ML (log β=6.11±0.19)
	Zn^{2+}	ML (log β=7.84±0.67)

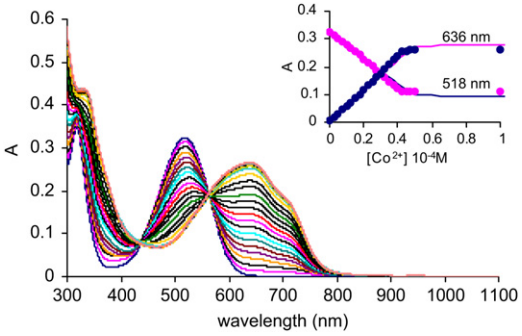

Figure 13. Effect of addition of Co^{2+} on UV–vis spectrum of **8** (50 μM; pH 7.0±0.1; CH_3OH/H_2O 1:1). Inset shows plot of absorbance at 518 nm and 636 nm on titration of **8** with Co^{2+}. The points refer to experimental values and line to curve fit.

Similarly, during the titration of **8** with Ni^{2+} the absorption band at 518 nm was attenuated while a new peak appeared at 666 nm (Fig. 14). Two clear isosbestic points at 442 nm and 594 nm indicate the formation of a well defined **8**-Ni^{2+} complex. The iterative spectral fitting of the data shows the formation of ML_2 (log β=12.6±0.8) and ML (log β=7.52±0.5) species.

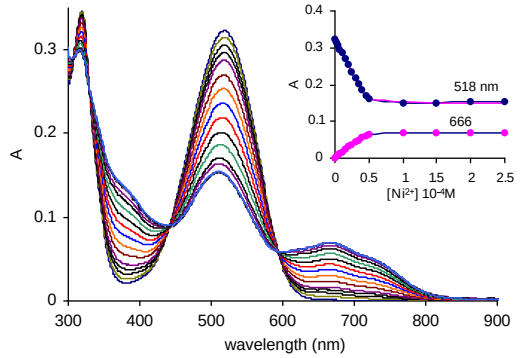

Figure 14. Effect of addition of Ni^{2+} on UV–vis spectrum of **8** (50 μM; pH 7.0±0.1; CH_3OH/H_2O 1:1). Inset shows plot of absorbance at 518 nm and 666 nm on titration of **8** with Ni^{2+}. The points refer to experimental values and line to curve fit.

During titration of chemosensor **8** with Cu^{2+}, the emergence of a new peak at λ_{max} 624 nm was observed. The concomitant decreases in absorbance at 518 nm on addition of Cu^{2+} with two isosbestic points at 430 nm and 560 nm was observed (Fig. 15). The iterative spectral fitting of the data shows that only ML (log β=7.27±0.37) species is formed.

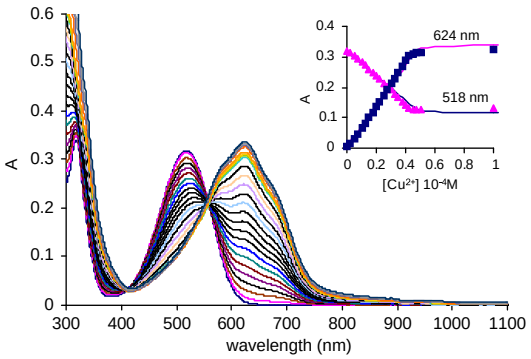

Figure 15. Effect of addition of Cu^{2+} on UV–vis spectrum of **8** (50 μM; pH 7.0±0.1; CH_3OH/H_2O 1:1). Inset shows plot of absorbance at 518 nm and 624 nm on titration of **8** with Cu^{2+}. The points refer to experimental values and line to curve fit.

The UV–vis titration of chemosensor **10** with Co^{2+} shows the formation of a new absorption band at 488 nm (Fig. 16) and the spectral fitting of the data converges the to the formation of ML (log β=7.65±0.3) and M_2L (log β=13.15±0.4) species. Similarly the titration of chemosensor **10** with Ni^{2+} shows the formation of new absorption band at 488 nm with two isosbestic points at 370 nm and 436 nm (Fig. 17). The spectral fitting of the results obtained

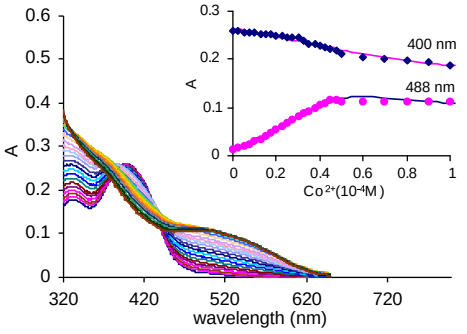

Figure 16. (a) Effect of addition of Co^{2+} on UV–vis spectrum of **10** (50 μM; pH 7.0±0.1; CH_3OH-/H_2O 1:1). Inset shows plot of absorbance at 400 nm and 488 nm on titration of **10** with Co^{2+}. The points refer to experimental values and line to curve fit.

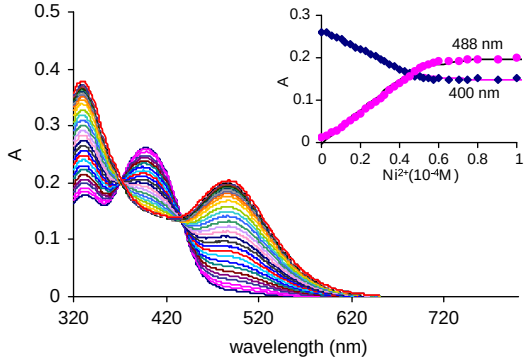

Figure 17. Effect of addition of Ni^{2+} on UV–vis spectrum of **10** (50 μM; pH 7.0±0.1; CH_3OH/H_2O 1:1). Inset shows plot of absorbance at 400 nm and 488 nm on titration of **10** with Ni^{2+}. The points refer to experimental values and line to curve fit.

from titration shows the formation of ML (log β=5.92±0.1). The titration of **10** with Cu^{2+} showed the formation of a new absorption band at 484 nm with two isosbestic points at 370 nm and 432 nm (Fig. 18). The spectral fitting showed the formation of ML (log β=6.11±0.2) species. Titration of **10** with Zn^{2+} under similar conditions showed the formation of a new blue shifted absorption band at 367 nm with an isosbestic point at 376 nm (Fig. 19). The spectral fitting shows the formation of ML complex (log β=7.78±0.6).

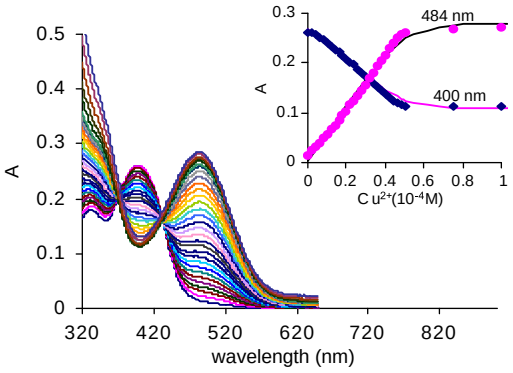

Figure 18. (a) Changes in the UV–vis spectrum of **10** (50 μM; pH 7.0±0.1; CH_3OH/H_2O 1:1) (b) Plot of absorbance of **10** upon titration with Cu^{2+}. The points refer to experimental values and line to curve fit.

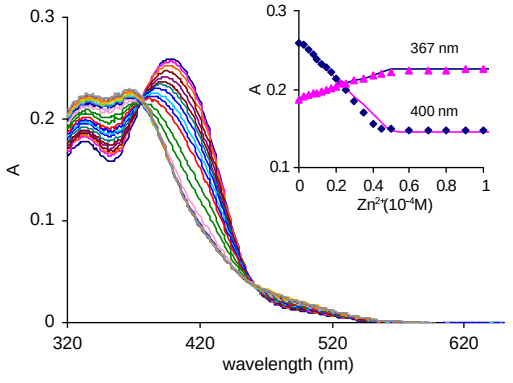

Figure 19. (a) Changes in the UV–vis spectra of **10** (50 μM; pH 7.0±0.1; CH_3OH/H_2O 1:1) (b) Plot of absorbance of **10** upon titration with Zn^{2+}. The points refer to experimental values and line to curve fit.

2.5. Ratiometric estimation of metal ions using chemosensors 2, 6, 8, and 10

The switching of λ_{max} values during addition of metal ions to chemosensors **2**, **6**, **8**, and **10** could be used to elaborate the ratiometric responses toward the metal ions. Ratiometric method increases the sensitivity and the dynamic range of the system and provides evaluation of metal ion independent of concentration of the chemosensor. Chemosensor **2** can be used to measure 5–150 μM with changing absorbance ratio A_{624nm}/A_{494nm} from 0.01 to 2.0, i.e., nearly 200 times increase in ratio (Fig. 20a). The higher binding stability of **6** toward Cu^{2+} shifts the lowest limit of Cu^{2+} estimation to 1 μM and highest 40 μM with nearly 60 times ratio change. Chemosensor **6** is significantly less sensitive to Co^{2+} and can measure Co^{2+} only 1–20 μM (Fig. 20b). Chemosensor **8** with an additional pyridine nitrogen as binding site shows nearly similar sensitivity to Cu^{2+} and Co^{2+} and is significantly less sensitive to Ni^{2+}. By using ratiometric approach chemosensor **8** (Fig. 20c) could measure 1–40 μM Co^{2+} with nearly 240 times ratio change but only

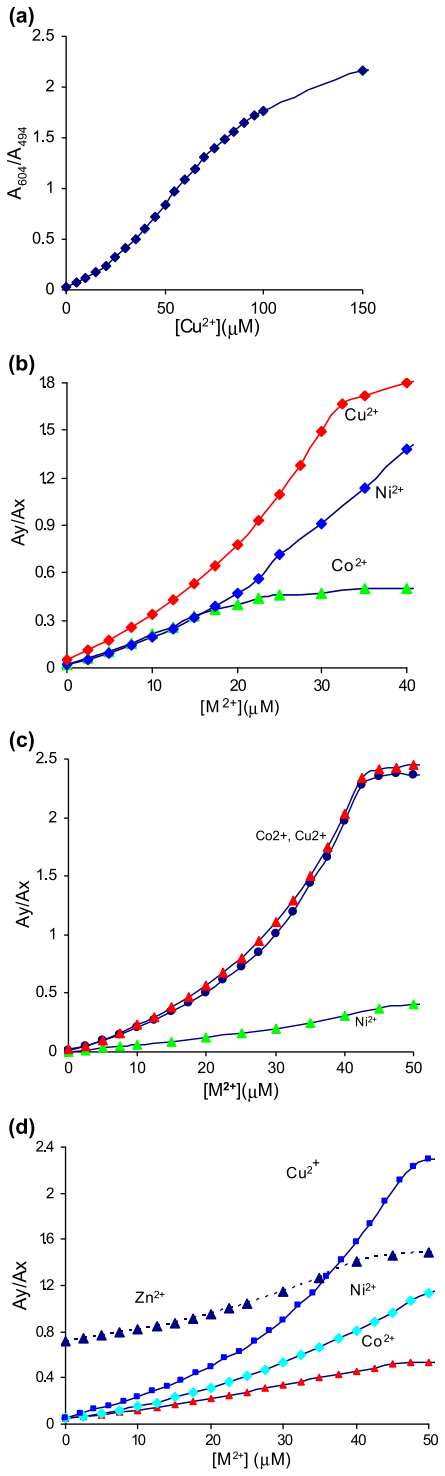

Figure 20. Ratiometric changes A_y/A_x in cases of chemosensors **2**, **6**, **8** and **10** on addition of various metal ions (a) chemosensor **2** (b) chemosensor **6**: A_{626}/A_{500} for Co^{2+}, and Ni^{2+}; A_{604}/A_{500} for Cu^{2+} (c) chemosensor **8**:A_{666}/A_{518} forNi^{2+}; A_{630}/A_{518} for Cu^{2+}, and Co^{2+} (d) Chemosensor **10**: A_{484}/A_{400} for Co^{2+}, Ni^{2+} and Cu^{2+}, and A_{367}/A_{400} for Zn^{2+}.

40 times change in ratio could be observed with Ni^{2+}. Chemosensor **10** with amide unit as binding site shows dual coordination mode for Co^{2+}, Ni^{2+}, Cu^{2+}, and Zn^{2+}.

Chemosensor **10** binds with Cu^{2+}, Ni^{2+}, and Co^{2+} in the order $Cu^{2+}>Ni^{2+}>Co^{2+}$ with least sensitivity for Co^{2+}. In ratiometric method, chemosensor **10** (Fig. 20d) could estimate 1 μM to 50 μM of metal ions with nearly 240 times ratio change in case of Cu^{2+}, 100 times ratio change in case of Ni^{2+} and only 30 times ratio change with Co^{2+}. There is just 20 times ratio change in case of Zn^{2+}.

3. Conclusions

Thus chemosensors **2**, **6**, **8**, and **10** depending on the nature and number of appended nitrogen atoms show highly selective to semi-selective behavior toward heavy metal ions. The conversion of sp^2 hybridised imine nitrogen in **2** to sp^3 hybridized alkylamine nitrogen in chemosensor **6** not only increases the binding with Cu^{2+} but also increases its sensitivity toward other metal ions. The dipicolylamine appendage, which is known to selectively complex with Zn^{2+} ions, allows binding of chemosensors **8** and **10** toward number of other metal ions. Further chemosensors **2** and **6** show only single mode for coordination but chemosensors **8** and **10** can bind with metal ions using both LMCT and ICT modes thus providing different color changes with different metal ions.

4. Experimental

4.1. General comments

Melting points were determined in open capillaries and are uncorrected. ^1H and ^{13}C NMR spectra were recorded on JEOL 300 MHz spectrometer using TMS as internal standard and $CDCl_3$ as solvent. FAB mass spectra were recorded on JEOL SX102 mass spectrometer using xenon (6 kV, 10 mA) as FAB gas. IR and CHN analysis were performed using Shimadzu FT-IR 8400S and Flash EA1112 CHNS-O analyzer, respectively. UV–vis spectra were recorded with Shimadzu UV-2450 spectrophotometer.

*4.1.1. Synthesis of 1-{2-[(2-pyridinylmethylene)amino] ethylamino}-anthracene-9,10-dione (**2**).* To a suspension of **1**[8a] (268 mg, 1 mmol) in ethanol (15 ml) was added pyridine-2-carboxaldehyde (127 mg, 1.2 mmol). The reaction mixture was stirred at room temperature for 12 h and the solid separated was filtered off to get pure **2**. Red solid; 80%; mp 160 °C (CH_3CN); [found C, 74.62; H, 5.12; N, 11.63. $C_{22}H_{17}N_3O_2$ requires C, 74.35; H, 4.82; N, 11.82%]; R_f (ethyl acetate) 0.19; ν_{max} (KBr) 1628, 1670, 1640 cm^{-1}; δ_H (300 MHz, $CDCl_3$): 3.76 (q, J=5.9 Hz, 2H, CH_2,), 4.04 (t, J=5.7 Hz, 2H, CH_2), 7.18 (d, J=7.8 Hz, 1H, ArH), 7.33–7.36 (m, 1H, ArH), 7.53–7.62 (m, 2H, ArH), 7.67–7.80 (m, 3H, ArH), 8.05 (d, J=8.1 Hz, 1H, ArH), 8.24 (t, J=7.4 Hz, 2H, ArH), 8.48 (s, 1H, CH), 8.64 (d, J=6.0 Hz, 1H, ArH), 9.98 (br s, 1H, NH, exchanges with D_2O); δ_C (75 MHz, $CDCl_3$): 43.4, 60.1, 113.4, 115.8, 117.9, 121.6, 124.9, 126.6, 126.7, 132.9, 133.0, 133.9, 134.7, 135.0, 135.2, 136.6, 149.5, 151.6, 154.2, 163.8, 183.4, 184.9; FAB mass M^+ m/z 356 (M^++1).

*4.1.2. General procedure for the synthesis of **6** and **8**.* To a solution of **3** (1.33 g, 5 mmol) in CH_2Cl_2 (75 ml) was added triethylamine (1.4 ml, 10 mmol) followed by methanesulphonyl chloride (0.53 ml, 7 mmol). The mixture was stirred at 40 °C. After completion of the reaction, mixture was extracted two times with dil HCl (2 N, 30 ml each portion). The organic phase was then washed with saturated sodium bicarbonate solution (30 ml) and then dried (Na_2SO_4). The solvent was distilled off to get pure **4**. To a solution of **4** (690 mg, 2 mmol) in CH_3CN (40 ml) were added K_2CO_3 (550 mg, 4 mmol) and 2-picolylamine **5** (130 mg, 2.4 mmol). The reaction mixture was stirred at 80 °C for 24 h. Then the reaction mixture was filtered off and washed with CH_3CN (20 ml) to get crude **6**. The crude product was then chromatographed on silica gel (100–200 mesh) to get pure **6**. Similarly, the reaction of **4** with di-(2-picolyl)amine gave **8**.

*4.1.2.1. Methanesulfonic acid 2-(9,10-dioxo-9,10-dihydro-anthracen-1-ylamino)-ethyl ester (**4**).* Red solid; 80%; mp 165 °C

(ethyl acetate); [Found: C, 60.25; H, 4.76; N, 4.36$C_{17}H_{15}NO_5S$ requires C, 59.12; H, 4.38; N, 4.06]; R_f(CHCl3) 0.35; ν_{max} ($CHCl_3$) 1625, 1665 cm^{-1}; δ_H (300 MHz, $CDCl_3$): 3.09 (s, 3H, CH_3), 3.77 (q, J=5.7 Hz, 2H, CH_2), 4.49 (t, J=5.7 Hz, 2H, CH_2), 7.10 (d, J=8.4 Hz, 1H, ArH), 7.56–7.81 (m, 4H, ArH), 8.24–8.30 (m, 2H, ArH); δ_C (75 MHz, $CDCl_3$): 37.7, 41.7, 67.2, 113.7, 116.5, 117.2, 126.7, 132.9, 133.2, 134.0, 134.6, 134.84, 135.5, 150.9, 166.7, 183.4, 185.4; FAB mass M^+ m/z 346 (M^++1).

*4.1.2.2. 1-{2-[(2-Pyridinylmethyl)amino]-ethylamino}-anthracene-9,10-dione (**6**).* Dark red solid; 65%; mp 135 °C (ethyl acetate); [found: C, 74.15; H, 5.76; N, 11.43. $C_{22}H_{19}N_3O_2$ requires C, 73.93; H, 5.36; N, 11.76%]; R_f (10% CH_3OH/CH_2Cl_2) 0.65; ν_{max} ($CHCl_3$) 1625, 1665 cm^{-1}; δ_H (300 MHz, $CDCl_3$): 3.06 (t, J=6.0 Hz, 2H, CH_2,), 3.50 (t, J=6.0 Hz, 2H, CH_2), 4.03 (s, 2H, CH_2), 7.08 (dd, J_1=8.7 Hz, J_2=1.2 Hz, 1H, ArH), 7.15–7.19 (m, 1H, ArH), 7.41 (d, J=7.8 Hz, 1H, ArH,), 7.50–7.61 (m, 2H, ArH), 7.66–7.79 (m, 3H, ArH), 8.25 (d, J=7.5 Hz, 1H, ArH), 8.29 (d, J=7.5 Hz, 1H, ArH), 8.54–8.56 (m, 1H, ArH), 9.91 (br s, 1H, NH, exchanges with D_2O); δ_C (75 MHz, $CDCl_3$): 42.6, 42.8, 54.6, 113.1, 115.7, 117.8, 122.1, 122.4, 126.6, 126.7, 132.8, 132.9, 133.8, 134.5, 134.9, 135.2, 136.5, 149.2, 151.5, 159.1, 183.7, 184.8; FAB mass M^+ m/z 358 (M^++1).

*4.1.2.3. 1-[[2-[Bis(2-pyridinylmethyl)amino]ethyl]amino]-anthracene-9,10-dione (**8**).* Dark red solid; 60%; mp 135 °C (ethyl acetate); [found: C, 74.76; H, 5.67; N, 12.65. $C_{28}H_{24}N_4O_2$ requires C, 74.98; H, 5.39; N, 12.49%]; R_f (10% CH_3OH/CH_2Cl_2) 0.45; ν_{max} ($CHCl_3$) 1630, 1672 cm^{-1}; δ_H (300 MHz, $CDCl_3$): 2.96 (t, J=6.0 Hz, 2H, CH_2), 3.45 (q, J=6.0 Hz, 2H, CH_2), 3.94 (s, 4H, CH_2), 6.94 (d, J=8.7 Hz, 1H, ArH), 7.13 (t, J=6.6 Hz, 2H, ArH), 7.47 (t, J=7.5 Hz, 1H, ArH,), 7.57 (d, J=7.5 Hz, 2H, ArH), 7.64 (t, J=7.5 Hz, 2H, ArH), 7.70–7.84 (m, 4H, ArH), 8.25 (d, J=7.5 Hz, 1H, ArH), 8.36 (d, J=7.5 Hz, 1H, ArH), 8.50 (d, J=5.1 Hz, 2H, ArH), 9.95 (br s, 1H, NH, exchanges with D_2O); δ_C NMR (75 MHz, $CDCl_3$): 40.4, 52.5, 60.6, 113.1, 115.6, 118.0, 122.1, 123.4, 126.6, 126.7, 132.9, 133.0, 133.9, 135.1, 136.6, 148.8, 151.3, 159.0, 183.9, 184.6; FAB mass M^+ m/z 448 (M^++1).

*4.1.3. Synthesis of 2-[bis(2-pyridinylmethyl)amino]-N-(9,10-dioxo-9,10-dihydro-anthracen-1-yl)-acetamide (**10**).* To a solution of 1-(chloroacetylamido)-anthracene-9,10-dione (**9**)[10] (600 mg, 2 mmol) in CH_3CN were added K_2CO_3 (550 mg, 4 mmol) and di-(2-picolyl)amine **7** (463 mg, 2.4 mmol). The reaction mixture was stirred at 80 °C for 24 h. After completion of the reaction, the suspended solid was filtered off and was washed with CH_3CN (20 ml). The solvent was removed under vacuum to get crude product. The crude product was chromatographed on silica gel (100–200 mesh) to get pure **10**; yellow solid; 75%; mp 195 °C (ethanol); [found: C, 72.76; H, 5.21; N, 12.45. $C_{28}H_{22}N_4O_3$ requires C, 72.71; H, 4.79; N, 12.11%]; R_f (ethyl acetate) 0.39; ν_{max} ($CHCl_3$) 1629, 1666, 1680 cm^{-1}; δ_H (300 MHz, $CDCl_3$): 3.54 (s, 2H, CH_2), 4.06 (s, 4H, CH_2), 7.16 (t, J=5.7 Hz, 2H, ArH), 7.64–7.77 (m, 3H, ArH), 7.85 (t, J=6.5 Hz, 2H, ArH), 7.96 (d, J=7.8 Hz, 2H, ArH), 8.08 (d, J=7.8 Hz, 1H, ArH), 8.31 (d, J=6.0 Hz, 1H, ArH) 8.39 (d, J=6.0 Hz, 1H, ArH), 8.53 (d, J=6.0 Hz, 2H, ArH), 9.16 (d, J=8.7 Hz, 1H, ArH), 13.1 (br s, 1H, NH, exchanges with D_2O); δ_C (75 MHz, $CDCl_3$): 59.5, 61.3, 118.3, 122.4, 123.6, 123.7, 126.4, 126.5, 127.1, 127.2, 132.9, 134.0, 134.2, 135.5, 136.6, 141.3, 149.0, 149.2, 157.9, 171.5, 182.8, 186.4; FAB mass M^+ m/z 463 (M^+).

4.2. Photophysical studies

UV–vis spectroscopy analysis was carried out on a Shimadzu UV-2450 PC UV–vis Spectrophotometer by using slit widths of 1.0 nm and matched quartz cells. All metal ion titrations were performed in CH_3OH/H_2O (1:1) at pH 7.0±0.1 (10 mM HEPES buffer). The pH—UV–vis combination titrations were performed in CH_3OH/H_2O (1:1) unbuffered solution. Stock solutions (0.1 M) of metal perchlorate salts were prepared in distilled water. Stock solutions (1 mM) of receptors were prepared in CH_3OH (**6**, **8**) and DMSO (**2**, **10**). UV–vis spectra were performed by using 50 μM solutions of receptors in CH_3OH/H_2O (1:1) and varying concentration of metal ions.

Metal binding features and affinity and stoichiometries of different complexes were assessed via titrations. Titration data is fit with programme specfit/32, which analyzes multi-wavelength data using an iterative method to obtain the association constant in terms of free or unbound metal ion.

Acknowledgements

We thank CSIR and DST, New Delhi for the financial assistance, UGC, New Delhi for CAS programme and CDRI Lucknow for FAB mass.

Supplementary data

Supplementary data associated with this article can be found in online version at doi:10.1016/j.tet.2010.06.031.

References and notes

1. (a) Fabrizzi, L.; Poggi, A. *Chem. Soc. Rev.* **1995**, 197–202; (b) De Silva, A. P.; Gunaratne, H. Q. N.; Gunnlaugsson, T.; Huxley, A. J. M.; McCoy, C. P.; Rademacher, J. T.; Rice, T. E. *Chem. Rev.* **1997**, *97*, 1515–1566; (c) Prodi, L.; Bolletta, F.; Montalti, M.; Zaccheroni, N. *Coord. Chem. Rev.* **2000**, *205*, 59–83; (d) Valeur, B.; Leray, I. *Coord. Chem. Rev.* **2000**, *205*, 3–40; (e) de Silva, A. P.; Fox, D. B.; Huxley, A. J. M.; Moody, T. S. *Coord. Chem. Rev.* **2000**, *205*, 41–57; (f) Rurack, K. *Spectrochim. Acta, Part A* **2001**, *57*, 2161–2195; (g) De Silva, A. P.; McCaughan, B.; McKinney, B. O. F.; Querol, M. *Dalton Trans.* **2003**, 1902–1913; (h) Callan, J. F.; De Silva, A. P.; Magri, D. C. *Tetrahedron* **2005**, *61*, 8551–8588.
2. (a) Beer, P. D.; Gale, P. A. *Angew. Chem., Int. Ed.* **2001**, *40*, 486–516; (b) Martinez-Manez, R.; Sancenon, F. *Chem. Rev.* **2003**, *103*, 4419–4476; (c) Fabbrizzi, L.; Licchelli, M.; Taglietti, A. *Dalton Trans.* **2003**, 3471–3479; (d) Martinez-Manez, R.; Sancenon, F. *J. Fluoresc.* **2005**, *15*, 267–285; (e) Gunnlaugsson, T.; Paduka Ali, H. D.; Glynn, M.; Kruger, P. E.; Hussey, G. M.; Pfeffer, F. M.; dos Santos, C. M. G.; Tierney, J. *J. Fluoresc.* **2005**, *15*, 287–299; (f) Martinez-Manez, R.; Sancenon, F. *Coord. Chem. Rev.* **2006**, *250*, 3081–3093; (g) Gunnlaugsson, T.; Glynn, M.; Tocci, G. M.; Kruger, P. E.; Pfeffer, F. M. *Coord. Chem. Rev.* **2006**, *250*, 3094–3117.
3. (a) Mierson, S. In *Handbook of Olfaction and Gustation*; Doty, R. L., Ed.; Marcel Dekker: New York, NY, 1995; pp 597–610; (b) Margolskee, R. F. In *Handbook of Olfaction and Gustation*; Doty, R. L., Ed.; Marcel Dekker: New York, NY, 1995; pp 575–595; (c) *Electronic Noses and Sensors for the Detection of Explosives*; Gardner, J. W., Yinon, J., Eds.NATO Science Series II: Mathematics, Physics and Chemistry; Kluwer Academic: Boston, 2004; Vol. 159; (d) Toko, K. *Sens. Actuators, B* **2000**, *64*, 205–215; (e) Albert, K. J.; Lewis, N. S.; Schauer, C. L.; Sotzing, G. A.; Stitzel, S. E.; Vaid, T. P.; Walt, D. R. *Chem. Rev.* **2000**, *100*, 2595–2626; (f) Jurs, P. C.; Bakken, G. A.; McClelland, H. E. *Chem. Rev.* **2000**, *100*, 2649–2678; (g) Lavigne, J. J.; Anslyn, E. V. *Angew. Chem., Int. Ed.* **2001**, *40*, 3118–3130.
4. Recent references on differential receptors: (a) Rakow, N. A.; Suslick, K. S. *Nature* **2000**, *406*, 710–713; (b) Drew, S. M.; Janzen, D. E.; Buss, C. E.; MacEwan, D. I.; Dublin, K. M.; Mann, K. R. *J. Am. Chem. Soc.* **2001**, *123*, 8414–8415; (c) Stojanovic, M. N.; Green, E. G.; Semova, S.; Nikic, D. B.; Landry, D. W. *J. Am. Chem. Soc.* **2003**, *125*, 6085–6089; (d) Paolesse, R.; Natale, C. D.; Nardis, S.; Macagnano, A.; D'Amico, A.; Pinalli, R.; Dalcanale, E. *Chem.—Eur. J.* **2003**, *9*, 5388–5395; (e) Wiskur, S. L.; Floriano, P. N.; Anslyn, E. V.; McDevitt, J. T. *Angew. Chem., Int. Ed.* **2003**, *42*, 2070–2072; (f) Garcia-Acosta, B.; Albiach-Marti, X.; Garcia, E.; Gil, L.; Martinez-Manez, R.; Rurack, K.; Sancenon, F.; Soto, J. *Chem. Commun.* **2004**, 774–775; (g) Suslick, K. S.; Rakow, N. A.; Sen, A. *Tetrahedron* **2004**, *60*, 11133–11138; (h) Baldini, L.; Wilson, A. J.; Hong, J.; Hamilton, A. D. *J. Am. Chem. Soc.* **2004**, *126*, 5656–5657; (i) Wright, A. T.; Anslyn, E. V.; McDevitt, J. T. *J. Am. Chem. Soc.* **2005**, *127*, 17405–17411; (j) Zhang, C.; Suslick, K. S. *J. Am. Chem. Soc.* **2005**, *127*, 11548–11549; (k) Zhou, H.; Baldini, L.; Hong, J.; Wilson, A. J.; Hamilton, A. D. *J. Am. Chem. Soc.* **2006**, *128*, 2421–2425; (l) Anslyn, E. V. *J. Org. Chem.* **2007**, *72*, 687–699; (m) Garcia-Acosta, B.; Martinez-Manez, R.; Sancenon, F.; Soto, J.; Rurack, K.; Spieles, M.; Garcia-Breijo, E.; Gil, L. *Inorg. Chem.* **2007**, *46*, 3123–3135; (n) Zhang, T.; Edwards, N. Y.; Bonizzoni, M.; Anslyn, E. V. *J. Am. Chem. Soc.* **2009**, *131*, 11976–11984; (o) Tomas, S.; Milanesi, L. *J. Am. Chem. Soc.* **2009**, *131*, 6618–6623; (p) Kitamura, M.; Shabbir, S. H.; Anslyn, E. V. *J. Org. Chem.* **2009**, *74*, 4479–4489.

5. (a) Raimundo, I. M.; Narayanaswamy, R. *Sens. Actuators, B* **2003**, *90*, 189–197; (b) Mikami, D.; Ohki, T.; Yamaji, K.; Citterio, D.; Ishihara, S.; Hagiwara, M.; Suzuki, K. *Anal. Chem.* **2004**, *76*, 5726–5733; (c) Komatsu, H.; Miki, T.; Citterio, D.; Kubota, T.; Shindo, Y.; Kitamura, Y.; Oka, K.; Suzuki, K. *J. Am. Chem. Soc.* **2005**, *127*, 10798–10799; (d) Komatsu, H.; Citterio, D.; Fujiwara, Y.; Minamihashi, K.; Araki, Y.; Hagiwara, M.; Suzuki, K. *Org. Lett.* **2005**, *7*, 2857–2859.
6. (a) Jimenez, D.; Martinez-Manez, R.; Sancenon, F.; Soto, J. *Tetrahedron Lett.* **2004**, *45*, 1257–1259; (b) Jimenez, D.; Martinez-Manez, R.; Sancenon, F.; Ros-Lis, J. V.; Soto, J.; Benito, A.; Garcia-Breijo, E. *Eur. J. Inorg. Chem.* **2005**, 2393–2403; (c) Schmittel, M.; Lin, H. W. *Angew. Chem., Int. Ed.* **2007**, *46*, 893–896.
7. (a) Xu, Z.; Qian, X.; Cui, J. *Org. Lett.* **2005**, *7*, 3029–3032; (b) Huang, J.; Xu, Y.; Qian, X. *Dalton Trans.* **2009**, 1761–1766; (c) Lu, C.; Xu, Z.; Cui, J.; Zhang, R.; Qian, X. *J. Org. Chem.* **2007**, *72*, 3554–3557.
8. (a) Kumar, S.; Kaur, N. *Supramol. Chem.* **2006**, *18*, 137–140; (b) Kaur, N.; Kumar, S. *Dalton Trans.* **2006**, 3766–3771; (c) Kaur, N.; Kumar, S. *Tetrahedron* **2008**, *64*, 3168–3175; (d) Kaur, N.; Kumar, S. *Tetrahedron Lett.* **2006**, 4109–4112; (e) Kaur, N.; Kumar, S. *Tetrahedron Lett.* **2008**, *49*, 5067–5069; (f) Kaur, N.; Kumar, S. *Chem. Commun.* **2007**, 3069–3070.
9. Ranyuk, E.; Douaihy, C. M.; Bessmertnykh, A.; Denat, F.; Averin, A.; Beletskaya, I.; Guilard, R. *Org. Lett.* **2009**, *11*, 987–990.
10. Ma, M.; Sun, Y.; Sun, G. *Dyes Pigm.* **2003**, *58*, 27–35.